



Preparation and Characterization of Multiwall Carbon Nanotubes

Decorated with Copper Oxide

Walaa M. Taha^{1*}, Mohamed Morsy^{2,4}, Nadra A. Nada¹ and Medhat A. Ibrahim^{3,4}



CrossMark

¹Physics Department, Faculty of Women for Arts, Science and Education, Ain Shams University, Cairo, 11757, Egypt

²Building Physics and Environment Institute, Housing & Building National Research Center (HBRC), 12311 Dokki, Giza, Egypt

³Molecular Spectroscopy and Modeling Unit, Spectroscopy Department, National Research Centre, 33 El-Bohouth St., Dokki, Giza 12622, Egypt

⁴Nanotechnology Research Centre (NTRC), The British University in Egypt (BUE), Suez Desert Road, El-Sherouk City, Cairo, 11837, Egypt.

Abstract

Multi-walled carbon nanotubes (MWCNTs) are special form of carbon nano materials with amazing applications in many areas of research. MWCNTs were synthesized by an Atmospheric Chemical Vapor Deposition (ACVD) system then decorated on their surface with Copper Oxide (CuO) nanoparticles via the hydrothermal method. The prepared un-purified MWCNTs and purified MWCNTs were characterized by High Resolution Transmittance Electron Microscope (HRTEM), X-ray Diffraction (XRD) and Raman spectroscopy. As well as the CuO/MWCNTs nanocomposite was characterized by HRTEM, XRD, Fourier Transform Infra-Red Spectroscopy (FTIR), Thermogravimetric Analysis (TGA) Differential Thermal Analysis (DTA) and Raman spectroscopy. The results demonstrated the distribution of CuO nano particles on the surface of MWCNTs as well as the particle size, which was around 43 nm. The prepared nanocomposite has high thermal stability with adequate well quality. The combination of CuO nanoparticles and MWCNTs gives rise to the production of a new composite with a wide range of applications.

Keywords: MWCNTs, CuO, Nanocomposite, TGA and XRD.

1. Introduction

In recent years, carbon nanotubes (CNTs) have become an interesting topic of scientific research due to their excellent remarkable properties of mechanical, electrical, chemical, and physical properties, as well as their high thermal stability and high surface area. These unique properties have directed CNTs toward a wide range of applications in several fields of nanoscience and nanotechnology [1-3]. MWCNTs are considered a concentric assembly series of (n) single wall carbon nanotubes (SWCNTs) where (n) higher than 2 and there is no limitation for the higher value [4,5]. Arc discharge, laser ablation, and chemical vapor deposition (CVD) are the three main methods for producing CNTs [6,7]. CVD seems to be the most suitable method for industrial use due to its high yield, high quality with different specific properties, and relatively low temperature unlike

other techniques. In addition, the CVD method offers an easy fabrication scale that harvests CNTs in different forms and shapes (powder, film, coiled, and straight) [8]. Synthesizing process of CNTs via CVD depends on the pyrolysis of hydrocarbon sources over a catalyst for the deposition of carbon cloud in a certain site in the furnace tube [9]. Since most of synthesizing methods of CNTs produce lots of impurities such as amorphous carbons, graphitic carbon, fullerenes, carbon onions and catalyst metals, the applications of CNTs depend on their purity [10]. Several techniques have been evolved for CNTs purification. Chemical purification techniques introduced oxygenated function groups such as carboxylic groups (-COOH) which is taken into consideration as serving the chemistry surface of nanotubes [11]. The catalyst particles can be removed by chemical purification during treatment with

*Corresponding author e-mail: walaataha505@gmail.com; (Walaa M. Taha).

Receive Date: 31 October 2021, Revise Date: 18 November 2021, Accept Date: 07 December 2021, First Publish Date: 07 December 2021

DOI: 10.21608/EJCHEM.2021.103677.4801

©2022 National Information and Documentation Center (NIDOC)

inorganic strong acids via refluxing or thermal treatment, which enhances the purification process [12]. Functionalization process plays an important role which facilitating loading nanoparticles on the CNTs surface and permits formation of several chemical function groups on CNTs surface [13,14]. Recently, researchers used molecular modelling to study theoretically the structure and properties of carbon nanomaterials. They are applying molecular modelling to understand the structure and behaviour of functionalization on nanotubes that lead to the well and suitable applications in many areas of research [15,16].

The combination of (CNTs) and nano particles (CNTs/NPs) leads to a successful integration of the properties of the two components in a new variety of applications [17,18]. The new composite (CNTs/NPs) has extraordinary new properties which combine the dual unique properties of CNTs and NPs. Meanwhile, the combination occurs by covalent or non-covalent bonds between the CNT surface and the covered nanoparticles(NPs)[17].This combination might be obtained by attaching NPs of metals (Ag, Au, Pt, Pd, Rh, etc.) to the external surface of CNTs [19]. Metal oxides (MOs) nanoparticles are also the most important and interesting class of material science. These MOs are formed on the CNTs surface as continuous amorphous, single crystalline films with discrete thickness and with different shapes and sizes such as nanorod, nanowire, etc [20].

Serious research has been developed to study the interactions of different MOs with CNTs surface. Mesoporous peapods were designed as $\text{Co}_3\text{O}_4/\text{CNT}$ electrode by using a controllable nano casting process. The new material offers high specific capacity, cyclic performance, and excellent rate capacity [21]. Researchers prepared a nanocomposite from ZnO/MWCNTs by using simple chemical methods during dip and dry process and by applying ionic layer reaction and adsorption. The electrochemical analysis of ZnO/MWCNTs showed the nanocomposite represented a good electrode for charge storage application [22]. Synthesized MWCNTs decorated with zinc oxide (ZnO) by using simple wet chemical route methods. They obtained ZnO with an average size of 30 nm and it has a high purity without any impurities [23]. CuO is P-type semiconductor that has band gap energy (1.2-1.7 eV). CuO is characterized by high chemical stability, easy synthesizing from several sources, low cost, nontoxic, and has a photocatalytic property. The main disadvantage of CuO is that it has a thin band gap, which causes recombination of the photogenerated (electrons-hole pairs) where the holes and electrons come back to each other quickly. The composite CuO/CNTs add interesting electrical, mechanical, chemical, and physical properties which solve numerous defects in pure CuO [24-26]. Khashan et al Studied the preparation and characterization of

decorated CNTs with different ratio of CuO nanoparticles by using laser ablation [27]. Yang et al Synthesized MWCNTs with CuO in nano leaves shape as plate form by using chemical precipitation methods. They observed that the nanocomposite has a remarkable property for glucose sensing [28].

In this study, MWCNTs were synthesized by ACVD system that produces a high yield of MWCNTs at a low cost. The MWCNTs were purified and functionalized via concentrated acid treatment. The distribution of CuO nanoparticles on the surface MWCNTs was achieved through the usage of hydrothermal treatment method where the most advantages of hydrothermal treatment method that produce uniform nanoparticles under controlling their size and shape. The prepared samples were characterized by different characterization techniques.

2. Experimental

2.1. Materials

Different chemicals and reagents were used for MWCNTs synthesizing, purification and decorations. Cobalt Nitrate hexa hydrate [$\text{Co}(\text{NO}_3)_2 \cdot 6\text{H}_2\text{O}$] was purchased from AlphaChemica. Iron Nitrate Nona hydrate [$\text{Fe}(\text{NO}_3)_2 \cdot 9\text{H}_2\text{O}$] was obtained from Guangdong Guangzhou Chemical Factory Co, Ltd. Magnesium Oxide [MgO] with purity of 99% from Prolabo Company. Sulfuric acid [H_2SO_4] was obtained from Scharlau, European Union. Nitric acid [HNO_3] was obtained from Caroer European Union. Cupric acetate monohydrate [$(\text{CH}_3\text{COO})_2\text{Cu} \cdot \text{H}_2\text{O}$] was obtained from LobaChemie. Ethanol [$\text{C}_2\text{H}_5\text{OH}$] was obtained from Chem-lab and Sodium hydroxide [NaOH] was purchased from Germany, EMD, Millipore corporation. All chemicals and reagents were used as it received without any further purification or treatment.

2.2. Synthesis of Materials

2.2.1. Catalyst Preparation

The bi-metallic Fe-Co Catalyst was prepared by the impregnation method. Firstly, 3.62 g of $\text{Fe}(\text{NO}_3)_2 \cdot 6\text{H}_2\text{O}$ and 2.47 g of $\text{Co}(\text{NO}_3)_2 \cdot 9\text{H}_2\text{O}$ were dissolved in 50 ml of distilled water then 10 g of MgO was added slowly under continuous stirring for 1 h at room temperature. Subsequently the mixture was dried at 120°C for 2 h. Eventually; the resultant catalyst was calcined at 550°C.

2.2.2. MWCNTs Synthesizing

MWCNTs were synthesized by using an APCVD system. The APCVD system consists of various tools, gas cylinders, and instruments, that were being carefully connected to each other to achieve safe and perfect operation. In a typical run, 0.5 g of fresh catalyst was placed inside the middle of reaction chamber. The furnace temperature was set at 750 °C,

meantime the nitrogen was allowed to flow at a rate of 30 ml/min. Once the required temperature is reached, acetylene gas is allowed to flow at a rate of 200 ml/min. The MWCNTs were deposited over catalytic particles for 30 min. Eventually, the Acetylene flow was interrupted, while keeping nitrogen flow continuously upon cooling to room temperature. The deposited carbonaceous material on the walls of quartz tube as a thin black film was collected.

2.2.3. MWCNTs Purification and Functionalization

1 g of un-purified MWCNTs were refluxed in 150 ml of 3:1 mixture of concentrated HNO_3 and H_2SO_4 solution, then sonicated in a water bath for 30 min. Subsequently, the mixture was continuously stirred for 2 h at 200°C, then left in the concentrated acid mixture at ambient conditions for additional 24 h. Thoroughly washed with distilled water several times until neutralization, then dried at 70°C for 24 h.

2.2.4. Synthesizing CuO/MWCNTs Nanocomposite:

The CuO NPs were grafted onto the external surface of MWCNTs by hydrothermal route. Two solutions were prepared separately and mixed then transferred to hydrothermal cell. 40 mg of MWCNTs were suspended in 50 ml absolute ethanol via ultrasonic for 30 min. A 300 mg of cupric acetate was dissolved in 50 ml ethanol at room temperature. The MWCNTs suspension was poured on cupric acetate solution then allowed to stir for an additional 1 h. The second solution is an oxidizer, containing 100 gm of NaOH in 50 ml of distilled water was added drop by drop to the above solution under continuous stirring for 4 h. Finally, the mixture was transferred to a 50 ml Teflon-lined sealed stainless-steel autoclave and maintained at 150°C under autogenous pressure for 4 h. The autoclave was cooled down naturally to room temperature, then washed thoroughly and calcinated at 350°C for 2 h.

2.3. Characterization Techniques

The shape and size of un-purified, purified MWCNTs and CuO/MWCNTs nanocomposite were studied by HRTEM JEM-2100.

The crystalline structure was determined by XRD diffractometer with a secondary monochromatic wavelength of Cu ($\lambda=1.542\text{\AA}$) at 45 K.V., 35 mA, and scanning speed of 0.02/sec.

Raman spectroscopy has been utilized to observe the structure and to confirm the SP^2 hybridization

state in the graphitic structure. The spectra were collected by (Bruker SENTERRA) with a (ND-YAG) laser source and with a wavelength of 532 nm.

Also, purified MWCNTs and CuO/MWCNTs nanocomposite was examined by TGA-DTA measurements by STDQ-600 thermal analyser from room temperature up to 1000°C under air atmosphere.

FTIR spectroscopy has been utilized to detect the functional groups on the surface of purified MWCNTs and the functional groups of nanoparticles on the surface of purified MWCNTs. The spectra were collected by (FTIR Vertex 70 Bruker optics model device).

Results and Discussion

2.4. MWCNTs Characterization

Figure 1 shows the HRTEM images of un-purified and purified MWCNTs. The HRTEM image of the un-purified MWCNTs shows that some catalyst particles are located at the end cap of MWCNTs. The catalyst particles appear as a dark spot. The location of the catalyst particles at the end of the cap suggests that the mechanism of reaction is root growth due to strong interaction between support catalyst (MgO) and metallic particles (Fe_2O_3 , CoO) [29]. The HRTEM micrograph of purified depicted in fig. 1 confirmed the hollow core structure of MWCNTs beside that the absence of amorphous carbon is clearly confirmed. The inner and outer diameter of MWCNTs were measured to be 6 nm and 25.7 nm respectively. After the purification process, the dark spots were absent this was due to the elimination of the catalyst particles.

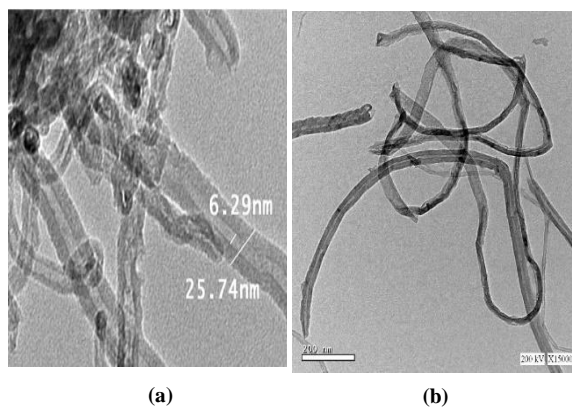


Fig. 1. HRTEM images of MWCNTs; a) before purification and b) after purification.

The XRD patterns of un-purified and purified MWCNTs are presented in figure 2. The diffraction peaks at $2\theta=26.3^\circ$ and 44.7° are indexed to (002) and (100) planes which are attributed to the hexagonal graphite structure. The structure of the MWCNTs has been confirmed using XRD measurements.

When compared to graphene, MWCNTs have (002) peak which might be weakly and broadened. Thus, asymmetric behaviour may be occurring due to the existence of multiple crystalline samples which consist of at least two crystalline sheets. Also, it is difficult to be isolated individually due to the graphite particles are stacked and wrapped in MWCNTs [30]. Therefore, the diffraction peaks of the XRD pattern of figure 2 confirm the formation of MWCNTs. The XRD pattern of un-purified MWCNTs exhibited sharp peaks at $2\theta = 38.3^\circ, 45^\circ, 62.3^\circ, 64.9^\circ$ and 78° . The diffraction peaks at $38.3^\circ, 45^\circ$ are indexed to (002) and (101) diffraction planes of MgO respectively. The diffraction peaks at $62.3^\circ, 64.9^\circ$ are assigned to (214) and (300) diffraction planes of iron oxide (Fe_2O_3) respectively. The diffraction peaks at $2\theta = 78^\circ$ corresponded to (222) and indicated to the presence of CoO. For purified MWCNTs the diffraction peaks of catalyst particles disappeared due to the purification process using strong acid. The characteristic diffraction peaks corresponding to the (002) plane was observed at $2\theta = 26.3^\circ$ and 25.9° for un-purified and purified MWCNTs respectively. This shift in peak position could be due to the removal of carbon impurities which existed between MWCNTs layers [31]. The XRD results confirm the formation of MWCNTs as proved by HRTEM.

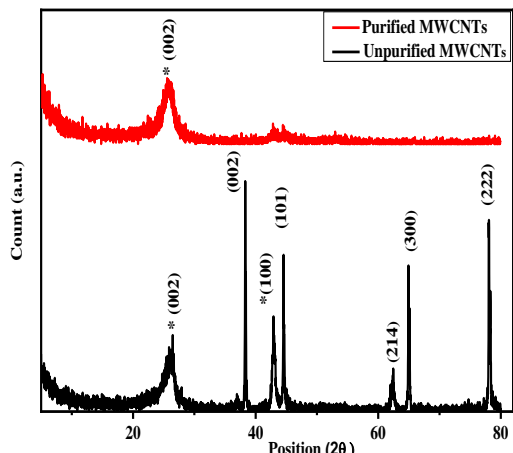


Fig. 2. XRD patterns of purified and un-purified MWCNTs.

The Raman spectra of figure 3 exhibits three Raman shifts for both un-purified and purified MWCNTs. The Raman shifts at $1566\text{cm}^{-1}, 1338\text{cm}^{-1}, 2677\text{cm}^{-1}$ is related to G, D, 2D bands respectively. The high energy mode is called G band and corresponds to the tangential vibrations of carbon atoms ($\text{C}=\text{C}$) which lie at 1566cm^{-1} , this band related to SP^2 hybridization of all carbon materials [32]. The G band for purified MWCNTs is sharper and narrower than for un-purified MWCNTs indicating the removal of catalyst particles, which resulted in inducing some defects to the outer surface of

MWCNTs [32,33]. The quality and purity of the crystalline structure of MWCNTs is obtained from the ratio of integrated intensities of D band and G band i.e. I_D/I_G [34]. It was known that, the higher crystalline lattice of nano tubes, the lower I_D/I_G ratio. The I_D/I_G for un-purified and purified MWCNTs sample equal to 0.85 and 0.6 respectively. The above mentioned results indicate that the un-purified MWCNTs have an inherent defects during their synthesizing. After purification the I_D/I_G decreased, which means that there is an improvement in the quality of the sample. In addition, the good advantage is that it is possible to obtain well purification without damage.

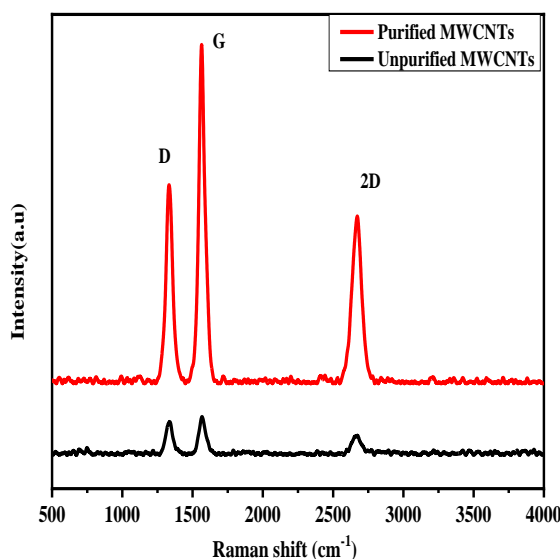


Fig. 3. Raman spectra of purified and un-purified MWCNTs.

2.5. Characterization of CuO/MWCNTs Nanocomposite

Figure 4 displays the HRTEM images of CuO/MWCNTs. The HRTEM images demonstrated that the CuO nanoparticles are attached to the external surface of MWCNTs. Additionally, CuO nanoparticles are coated on the tubular structure of nanotubes with strong adhesion between the CuO nanoparticles and MWCNTs.

The XRD diffraction pattern of CuO/MWCNTs is presented in figure 5. The diffraction peaks at $2\theta = 26^\circ$ and 43.6° are indexed to (002) and (100) planes of MWCNTs respectively as elucidated earlier in fig. 2. The characteristic peaks at $2\theta = 35.7^\circ, 38.4^\circ, 61.3^\circ$ and 74° are indexed to (-111), (111), (113) and (311) are due to the monoclinic structure of CuO phase [35]. The pattern at $2\theta = 44^\circ$ and 50.9° are corresponding to the cubic phase of Cu [36]. No additional peaks belonging to any impurities were detected in the XRD diffraction patterns demonstrated the high purity of CuO/MWCNTs nanocomposite. The particle size of CuO nanoparticles was estimated by

Debby Scherrer's equation and found to be about 43 nm [37].

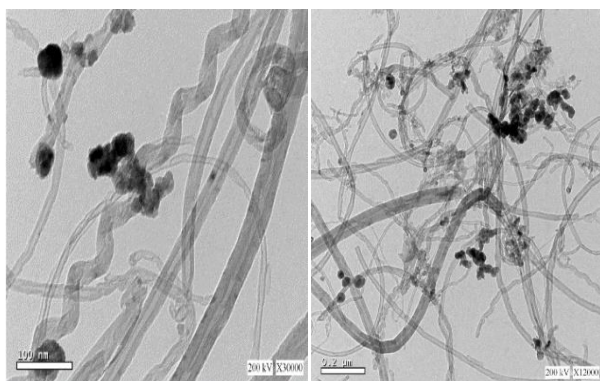


Fig.4. HRTEM images of CuO/MWCNTs nanocomposite.

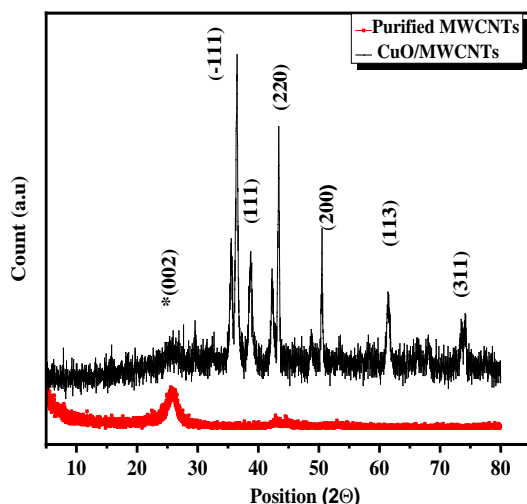


Fig. 5. XRD pattern of CuO/ MWCNTs and purified MWCNTs.

The FTIR spectra of the CuO/MWCNTs nanocomposite confirm the presence of CuO on the surface of MWCNTs as depicted in figure 6. The broad band at 3435 cm^{-1} associated with the stretching of $-\text{OH}$ group of adsorbed water. The bands at 2858 cm^{-1} - 2924 cm^{-1} are assigned to asymmetric and symmetric stretching vibration of C-H in $-\text{CH}_3$ and CH_2 group respectively. The band at 1628 cm^{-1} associated with $\text{C}=\text{C}$ of SP^2 hybridization in nanotubes ring [38]. The band at $1115\text{--}1060\text{ cm}^{-1}$ attributed to C-O stretching vibrations in the carboxylic groups[39]. The band at 1714 cm^{-1} which refers to $\text{C}=\text{O}$ in the carboxylic groups and the two bands at 1115 cm^{-1} - 1060 cm^{-1} attributed to C-O. It was

recognized that the carboxylic group is removed by the reduction reaction. However, due to the low reducibility of Cu^+ there are some epoxy group or hydroxy group present on MWCNTs surface which cause an increase in C-O stretching vibration bands. This reason confirms the reduction of MWCNTs by cuprous ions to form CuO nanoparticles [40]. Swamwar NV et al in 2012 confirm that the characteristic peaks of Cu-O appear at $400\text{--}600\text{ cm}^{-1}$ [41]. In this spectra, the additional observed bands at 447 cm^{-1} , 606 cm^{-1} is due the stretching vibration mode of Cu-O in the monoclinic structure of CuO.

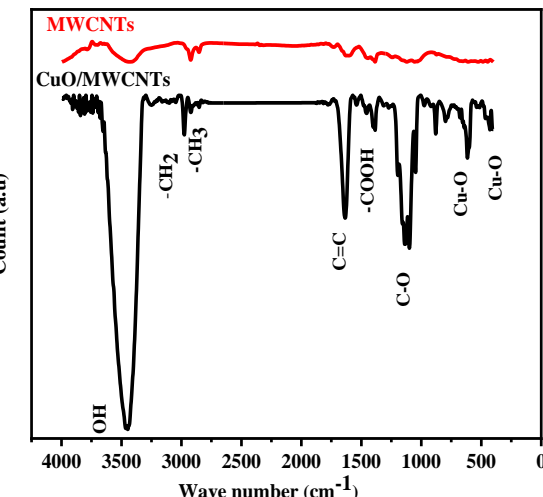


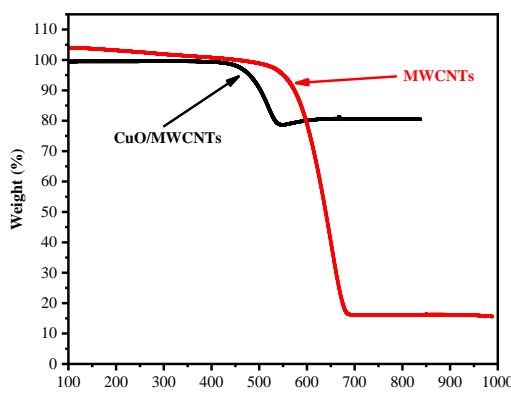
Fig. 6. FT-IR spectra of Purified MWCNTs and CuO/MWCNTs nanocomposite.

The thermal analysis (TGA and DTA) curves of purified MWCNTs and CuO/MWCNTs nanocomposite are presented in figures 7a and 7b respectively.

The TGA curve of purified MWCNTs exhibits residual weight due to the presence of some metallic particles in the carbon cage or between the inter shell layers of MWCNTs. It is so difficult to remove the metallic particles residue because of the graphitic structure is highly resistant to the oxidation process. Therefore, any influence of additional oxidation may cause damage to MWCNTs surface [42]. However, the purified MWCNTs have high purity, high thermal stability, and fewer defects as confirmed earlier by HRTEM and XRD measurements. The DTA thermogram of the purified MWCNTs is characterized by an endothermic peak from $532\text{ }^\circ\text{C}$ to $711\text{ }^\circ\text{C}$.

The TGA curves of the nanocomposite CuO/MWCNTs showed weight loss of about 22% which is attributed to the oxidation of MWCNTs. The amount of CuO nano particles were estimated from TGA measurement. The loading ratio was estimated to be 78% of CuO on the surface of MWCNTs. The DTA curve for CuO/MWCNTs showed an endothermic peak at 523 °C which refers also to the oxidation of MWCNTs. It was shown that the oxidation temperature of MWCNTs was shifted toward lower temperature might be because of the catalytic role of CuO, presence of NaOH in solution, and the effect of hydrothermal treatment. The results showed good agreement with HRTEM, XRD and FTIR measurements.

Fig. 7a. TGA curves of purified MWCNTs and CuO/MWCNTs



nanocomposite

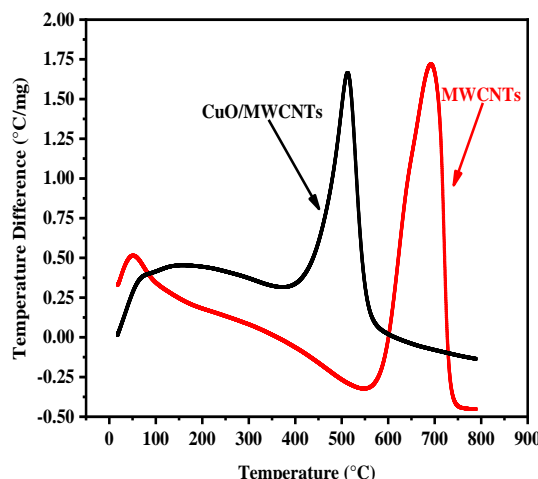


Fig. 7b. DTA curves of purified MWCNTs and CuO/MWCNTs nanocomposite.

The Raman spectra of CuO/MWCNTs is illustrated in figure 8. The Ramanshifts around 1566cm^{-1} , 1338cm^{-1} , and 2677cm^{-1} corresponded to G (the graphite band), D (disorder band), and 2D (second order harmonic) bands of MWCNTs

respectively. According to group theory, there are three Raman active modes of CuO, at 228cm^{-1} , 333cm^{-1} and 697cm^{-1} corresponding to one A_g , and two B_g modes which are related to the vibration modes of CuO structure[43]. The I_D/I_G of CuO /MWCNTs is 0.9 which is higher than purified MWCNTs (0.6). This means that there are some defects that affect the graphitic structure of MWCNTs. Increasing D, G intensities are related to the partial reduction of MWCNTs when they are decorated with CuO[43, 44, 45, 46]. The above results confirm the presence of CuO on MWCNTs surface. Fig. 8. Raman spectra of CuO/ MWCNTs nanocomposite and purified MWCNTs.

4. Conclusion

In this work, the MWCNTs were synthesized by the APCVD system. The CuO nano particles were attached to the external surface of MWCNTs via hydrothermal route. The purified MWCNTs and CuO/MWCNTs nanocomposites were characterized using different techniques including XRD, HRTEM, FTIR, DTA, TGA and Raman. The results obtained by the above-mentioned characterization techniques confirmed the successive functionalization process of MWCNTs where XRD confirms the elimination of the catalytic particles from MWCNTs surface. The FTIR proved the formation of carboxyl groups on the MWCNTs surface. The CuO/MWCNTs nanocomposite was synthesized by hydrothermal route. The HRTEM demonstrated the presence of CuO nanoparticles on outer surface of MWCNTs. The particle size of CuO was calculated by Debye Scherrer's equation and found to be 43nm. The TGA-DTA demonstrated the high thermal stability of nanocomposite. Raman spectra confirm the presence of CuO nanoparticles where the characteristic three modes ($A_g, 2B_g$) of CuO are observed.

5. Conflicts of interest

"There are no conflicts to declare".

References

- [1] Eatemadi, A., Daraee, H., Karimkhanloo, H., Kouhi, M., Zarghami, N., Akbarzadeh, A., Abasi, M., Hanifehpour, Y. and Joo, S.W., Carbon nanotubes: properties, synthesis, purification, and medical applications. *Nanoscale research letters*, 9(1), 1-13 (2014).
- [2] Pandey, P. and Dahiya, M., Carbon nanotubes: Types, methods of preparation and applications. *International Journal of Pharmaceutical Science and Research* 1(4), 15-21 (2016).
- [3] Ibrahim, K.S., Carbon nanotubes-properties and applications: a review. *Carbon letters*, 14(3), 131-144 (2013).
- [4] Krueger A., Monthioux and M., *Strained hydrocarbons in carbon nanotubes, Beyond the van-t Hoff and Le Bel*

- Hypothesis* Ed. Dodziuk H. Chap. 6, Wiley-VCH Verlag, 335(2009).
- [5] Ghaffoori, A.J. and Abdul-Adheem, W.R., A Review on Carbon Nanotubes Structural Types and Techniques. *Journal of Al-Ma'moon College*, 1(34), 346-378 (2019).
- [6] Prasek, J., Drbohlavova, J., Chomoucka, J., Hubalek, J., Jasek, O., Adam, V. and Kizek, R., Methods for carbon nanotubes synthesis. *Journal of Materials Chemistry*, 21(40), 15872-15884 (2011).
- [7] Dai, H., Carbon nanotubes: synthesis, integration, and properties. *Accounts of chemical research*, 35(12), 1035-1044 (2002).
- [8] Kumar, M. and Ando, Y., Chemical vapor deposition of carbon nanotubes: a review on growth mechanism and mass production. *Journal of nanoscience and nanotechnology*, 10(6), 3739-3758 (2010).
- [9] Hussein, F.H., and Abdulrazzak, F.H., Synthesis of carbon nanotubes by chemical vapor deposition. *Nanomaterials: Biomedical, Environmental, and Engineering Applications*, Ch. 4. Wiley(2018).
- [10] Mohammed, M.K., Radhi, I.M., Yas, D.A., Abbas, A.M. and Abdulrazzak, F.H., Purification and functionalization of carbon nanotubes based on hydrogen peroxide. *International Journal of Advanced Biotechnology and Research*, 8(3), 2345-2351 (2017).
- [11] Díez-Pascual, A.M., Chemical functionalization of carbon nanotubes with polymers: A Brief Overview. *Macromol*, 1(2), 64-83 (2021).
- [12] Dillon, A.C., Gennett, T., Jones, K.M., Alleman, J.L., Parilla, P.A. and Heben, M.J., A simple and complete purification of single-walled carbon nanotube materials. *Advanced Materials*, 11(16), 1354-1358 (1999).
- [13] Salah, L.S., Ouslimani, N., Bousba, D., Huynen, I., Danlée, Y. and Aksas, H., Carbon nanotubes (CNTs) from synthesis to functionalized (CNTs) using conventional and new chemical approaches. *Journal of Nanomaterials*, 2021, 31 (2021).
- [14] Chavali, M.S., and Nikolova, M.P., Metal oxide nanoparticles and their applications in nanotechnology. *SN Applied Sciences*, 1(6), 1-30 (2019).
- [15] Ezzat, H.; Ibrahim, M; and Elhaes H., Molecular modeling applied for carbon nano materials. *Egyptian Journal of Chemistry*, 63(12), 4777-4787 (2020).
- [16] Elhaes H., Ezzat H., Badry R., Yahia I.S., Zahran H.Y., Ibrahim M. A, The interaction between carbon nanotube decorated with CuO and ZnO and hydrogen, *Sensor Letter*, 16(6), 445-353(2018).
- [17] Dobrzańska-Danikiewicz, A., Łukowiec, D., Cichocki, D. and Wolany, W., Carbon nanotubes decorating methods. *Archives of Materials Science*, 54, 53-61 (2013).
- [18] Dighole, R.P., Munde, A.V., Mulik, B.B. and Sathe, B.R., Bi₂O₃nanoparticles decorated carbon nanotube: An effective nanoelectrode for enhanced electrocatalytic 4-Nitrophenol reduction. *Frontiers in Chemistry*, 8, 325(2020).
- [19] Georgakilas, V., Gournis, D., Tzitzios, V., Pasquato, L., Guldi, D.M. and Prato, M., Decorating carbon nanotubes with metal or semiconductor nanoparticles. *Journal of Materials Chemistry*, 17(26), 2679-2694(2007).
- [20] Charitidis, C.A., Georgiou, P., Koklioti, M.A., Trompeta, A.F. and Markakis, V., Manufacturing nanomaterials: from research to industry. *Manufacturing Review*, 1, 11(2014).
- [21] Gu, D., Li, W., Wang, F., Bongard, H., Spliethoff, B., Schmidt, W., Weidenthaler, C., Xia, Y., Zhao, D. and Schüth, F., Controllable synthesis of mesoporous peapod-like Co₃O₄@ carbon nanotube arrays for high-performance lithium-ion batteries. *Angewandte Chemie*, 127(24), 7166-7170 (2015).
- [22] Sankpal, B.R., Gajare, H.B., Karade, S.S., Salunkhe, R.R. and Dubal, D.P., Zinc oxide encapsulated carbon nanotube thin films for energy storage applications. *Electrochimica Acta*, 192, 377-384 (2016).
- [23] Morsy, M., Helal, M., El-Okr M., and Ibrahim M., Preparation and characterization of multiwall carbon nanotubes decorated with zinc oxide. *Der Pharma Chemica*, 7(10), 139-144 (2015).
- [24] Devi, L.V., Sellaiyan, S., Selvalakshmi, T., Zhang, H.J., Uedono, A., Sivaji, K. and Sankar, S., Synthesis, defect characterization and photocatalytic degradation efficiency of Tb doped CuOnanoparticles. *Advanced Powder Technology*, 28(11), 3026-3038 (2017).
- [25] Ramesh, M., CuO as efficient photo catalyst for photocatalytic decoloration of wastewater containing Azo dyes. *Water Practice & Technology*, 16(4), 1078-1090 (2021).
- [26] Sonia S., Poongodi, S., Kumar P.S., MangalarajD., Ponpandian N., and Viswanathan, C., Hydrothermal synthesis of highly stable CuO nanostructures for efficient photocatalytic degradation of organic dyes. *Materials Science in Semiconductor Processing*, 30, 585-591 (2015).
- [27] Khashan K.S., Jabir, M.S. and Abdulameer, F.A., May. Preparation and characterization of copper oxide nanoparticles decorated carbon nanoparticles using laser ablation in liquid. *Journal of Physics: Conference Series* 1003(1), 12100 (2018).
- [28] Yang Z., Feng, J., Qiao J., Yan, Y., Yu, Q. and Sun, K., Copper oxide nanoleaves decorated multi-walled carbon nanotube asplatform for glucose sensing. *Analytical Methods*, 4(7), 1924-1926 (2012).
- [29] Belin T., and Epron F., Characterization methods of carbon nanotubes: a review. *Materials Science and Engineering: B*, 119(2), 105-118(2005).
- [30] Das R., Bee A. S., EaquibA.M., Ramakrishna S., and Yongzhi, W., Carbon nanotubes characterization by X-ray powder diffraction-Areview. *Current Nanoscience*, 11(1), 23-35(2015).
- [31] Charlier A., McRae E., Heyd, R., Charlier M.F., and Moretti, D., Classification for double-walled carbonnanotubes. *Carbon*, 37(11), 1779-1783(1999).
- [32] DiLeo, R.A., Landi, B.J. and Raffaelle, R.P., Purity assessment of multiwalled carbon nanotubes by Raman spectroscopy. *Journal of applied physics*, 101(6), 064307(2007).
- [33] Murphy, H., Papakonstantinou P., and Okpalugo T.T., Raman study of multiwalled carbon nanotubes functionalized with oxygen groups. *Journal of Vacuum Science & Technology B: Microelectronics and Nanometer Structures Processing, Measurement, and Phenomena*, 24(2), 715-720 (2006).
- [34] Shen, G., Bando, Y. and Lee, C.J., Synthesis and evolution of novel hollow ZnO urchins by a simple

- thermal evaporation process. *The Journal of Physical Chemistry B*, 109(21),10578-10583 (2005).
- [35] Mahmoodi, N.M., Rezaei, P., Ghotbei, C. and Kazemeini M., Copper oxide-carbon nanotube (CuO/CNT) nanocomposite: Synthesis and photocatalytic dye degradation from colored textile wastewater. *Fibers and Polymers*, 17(11), 1842-1848(2016).
- [36] Zhao Y., Song X., Song Q. and Yin, Z., A facile route to the synthesis copper oxide/reduced graphene oxide nanocomposites and electrochemical detection of catechol organic pollutant. *CrystEngComm*, 14(20),6710-6719(2012).
- [37] Chen C.S., Chen, X.H., Yi B., Liu, T.G., Li, W.H., Xu, L.S., Yang, Z., Zhang H., and Wang, Y.G., Zinc oxide nanoparticle decorated multi-walled carbon nanotubes and their optical properties. *Acta Materialia*, 54(20), 5401-5407 (2006).
- [38] Moreno-Castilla, C., Carrasco-Marin, F., Maldonado-Hodar, F.J. and Rivera-Utrilla, J., Effects of non-oxidant and oxidant acid treatments on the surface properties of an activated carbon with very low ash content. *Carbon*, 36(1-2), 145-151(1998).
- [39] Nasiri, A., Shariaty-Niasar, M., Rashidi, A.M. and Khodafarin, R., Effect of CNT structures on thermal conductivity and stability of nanofluid. *International Journal of heat and Mass transfer*, 55(5-6), 1529-1535(2012).
- [40] DehnoKhalaji, A., Jafari, K. and Maghsodlou Rad, S., Solid-state thermal decomposition method for the preparation of CuO nanoparticles. *Journal of Nanostructures*, 2(4), 505-508 (2012).
- [41] Suramwar, N.V., Thakare, S.R. and Khaty, N.T., Synthesis and catalytic properties of nano CuO prepared by soft chemical method. *International Journal of Nano Dimension*, 3(1), 75-80 (2012).
- [42] Dresselhaus, M.S., Jorio, A., Hofmann, M., Dresselhaus, G. and Saito, R., Perspectives on carbon nanotubes and graphene Raman spectroscopy. *Nano letters*, 10(3),751-758(2010).
- [43] Zdrojek, M., Gebicki, W., Jastrzebski, C., Melin, T. and Huczko, A., Studies of multiwall carbon nanotubes using Raman spectroscopy and atomic force microscopy. *Solid State Phenomena*, 99, 265-268 (2004).
- [44] Ghaedi M., Shokrollahi A., Tavallali H., hojaiepoor F., Keshavarz B., Hossainian H., Soylak M., andPurkait M.K., Activated carbon and multiwalled carbon nanotubes as efficient adsorbents for removal of arsenazo(III) and methyl red from waste water. *Toxicological and Environmental Chemistry*, 93(3), 438-449 (2011).
- [45] Soylak M., andSahinbas D. H., Copper, iron, and lead levels in fertilizer and water samples: separation and preconcentration on multiwaled carbon nanotubes. *Desalination and Water Treatment*,51(37-39) 7296-7303 (2013)
- [46] Duran A., TuzenM.,andSoylakM.,Separation and Enrichment of Gold in Water, Geological and Environmental Samples by Solid Phase ExtractiononMultiwalled Carbon Nanotubes Prior to its Determination byFlame Atomic Absorption Spectrometry. *Journal of AOAC International*98(6) 1733 – 1738 (2015).